SUPPLEMENTAL MATERIAL

A-Gonzalez et al., https://doi.org/10.1084/jem.20161375

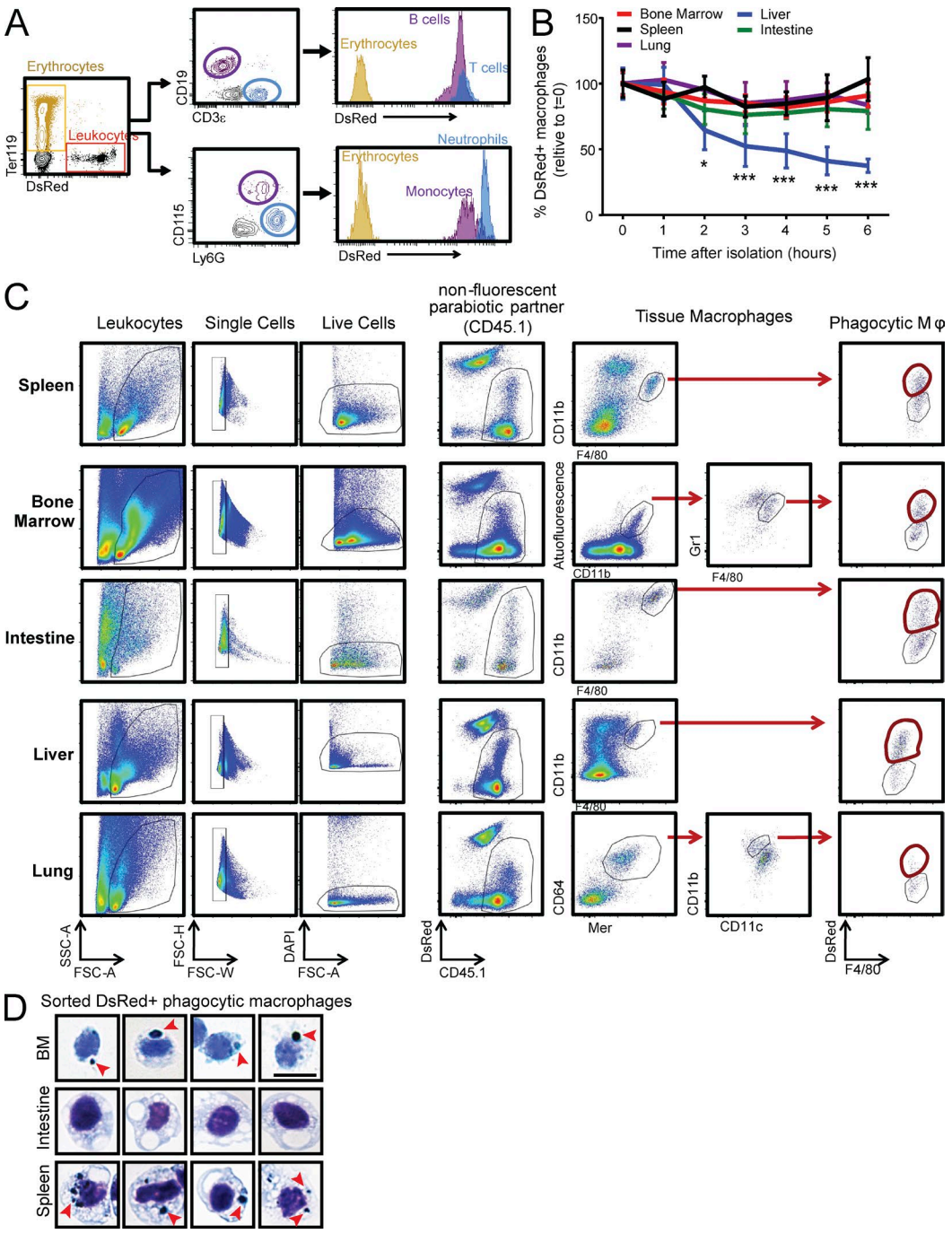

Figure S1. **Characterization of target cells and phagocytic and nonphagocytic macrophages.** (A) Representative FACS plots of blood from DsRed-Tg mice showing expression of DsRed on all leukocyte subsets but no on erythrocytes (Ter119+SSC-A^{low} cells). *n* = 3 mice. (B) Kinetics of degradation of DsRed^{+} signal within macrophages from the indicated tissues, measured by flow cytometry. Time 0 corresponds to the time when tissues were extracted from mice, and maintained at 37°C until analysis. Data show mean ± SEM from three mice. *, P > 0.05; ***, P > 0.001, as determined by Student's *t* test analysis relative to t = 0 for each tissue. *n* = 7 pairs from three independent experiments. (C) Cytometry plots showing the strategy followed for the identification of tissue-resident macrophages in multiple tissue of CD45.1-WT: DsRed-Tg parabionts. After at least 8 wk in parabiosis, tissues from the nonfluorescent CD45.1 partner were processed for flow cytometry and macrophages identified following the labeling and gating strategies shown for each set of plots. Phagocytic macrophages were identified on the basis of incorporation of DsRed^{+} material into CD45.1 nonphagocytic cells (dotted region in the far right plots). (D) Representative phagocytic (DsRed^{+}) macrophages sorted from the bone marrow, spleen, and intestine of parabiotic mice, cytospun, and stained with Giemsa. Red arrows point to what appear to be ingested material in bone marrow and spleen, whereas intestinal macrophages show large vacuoles. *n* = 10 pairs from four independent experiments.

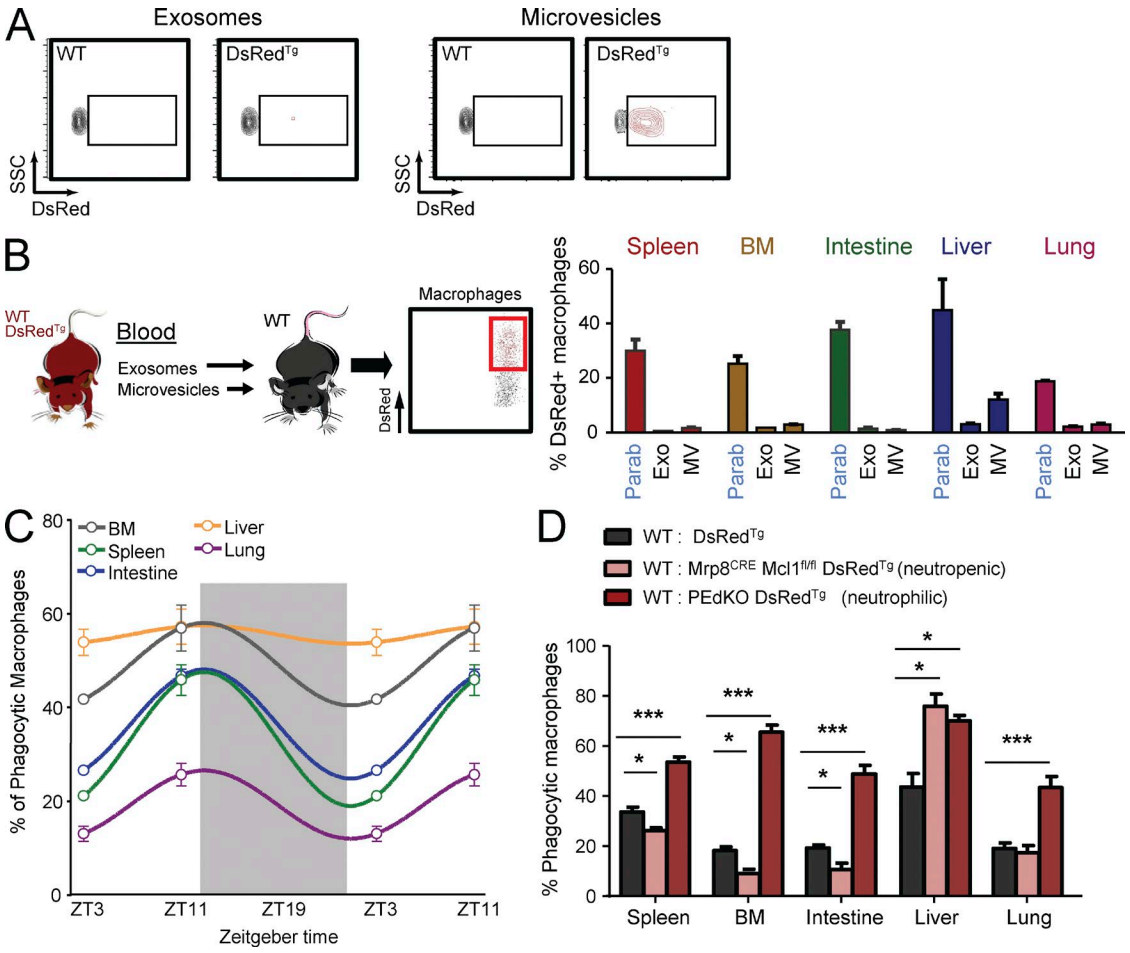

Figure S2. **Characterization of phagocytosed material, circadian patterns of phagocytosis, and preferential engulfment of neutrophils.** (A) Representative cytometry plots of beads conjugated with exosomes or microvesicles, demonstrating fluorescence only associated with microvesicles. (B) Experimental strategy: exosomes and microvesicles prepared from the blood of DsRed-Tg mice were transferred into nonfluorescent mice. Bars show the percentage of macrophages that took up fluorescence; the levels in parabionts for each tissue are shown for comparison. $n = 4$ animals per group from one experiment. (C) Cosinor-based plots (adjusted to 24-h cycles; Cornelissen, 2014) displaying the predicted oscillatory frequency of phagocytic macrophages in different tissues over time. The shaded rectangle indicates night. Data were extrapolated from analyses at ZT3 and ZT11; $n = 6$ per group from two independent experiments. (D) Percentage of phagocytic macrophages across the indicated tissues of wild-type (nonfluorescent) mice set in parabiosis with DsRed^{Tg} control mice, with mice that lack circulating neutrophils (Mrp8^{CRE} Mcl1$^{fl/fl}$; Dzhagalov et al., 2007) or with mice that are neutrophilic (deficient in endothelial selectins; PEdKO mice; Frenette et al., 1996). Both neutrophil-deficient and neutrophilic mice expressed the DsRed transgene to allow identification of phagocytic cells, thus allowing determination of the contribution of neutrophils as targets of phagocytosis; $n = 3$–6 mice per group from three independent experiments. Note that only the liver fails to display rhythmicity of phagocytosis and correlations with neutrophil numbers in blood. Plots and bars show mean ± SEM. *, $P < 0.05$; ***, $P < 0.001$ as determined by unpaired Student's t test.

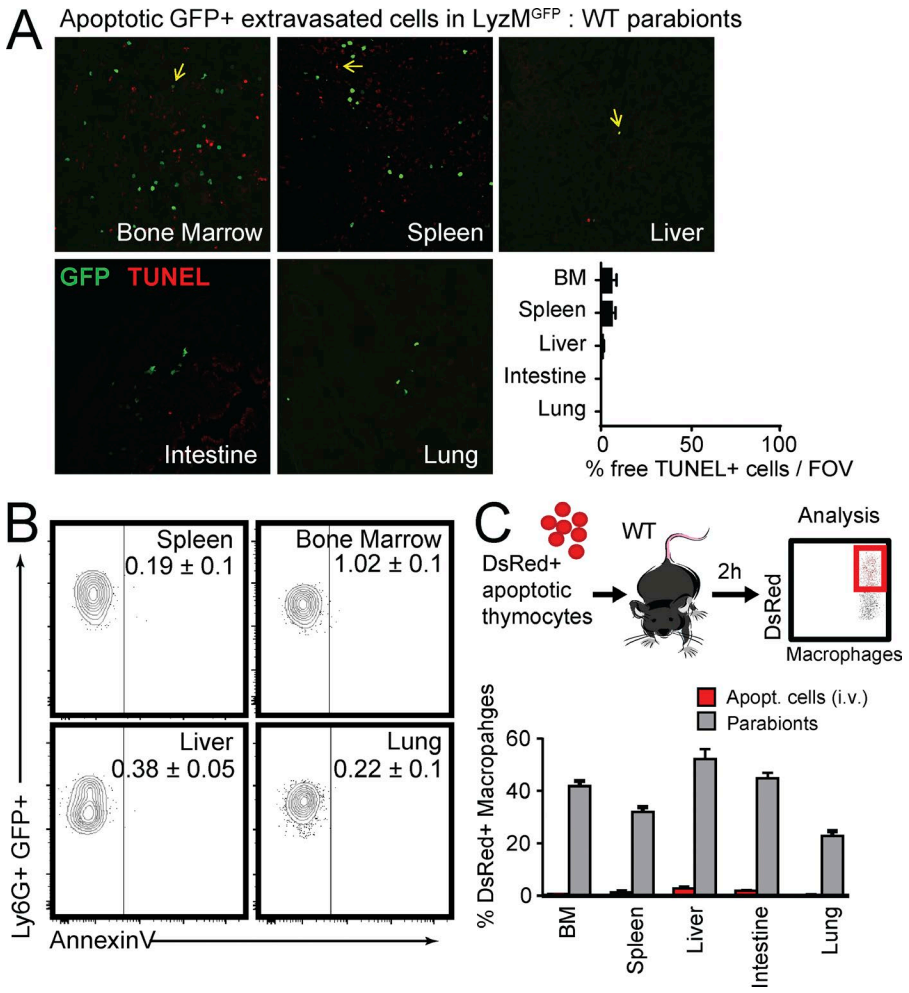

Figure S3. **Apoptosis of target cells in tissues is rare and not sufficient for phagocytosis.** (A) Representative images of TUNEL$^+$ GFP^{HI} neutrophils in tissue sections of wild-type mice in parabiosis with LysM-GFP partner mice. Yellow arrows show double-positive cells, which are quantified in the bar graph as the percentage of GFP^{HI} cells that are TUNEL$^+$. Data are from 7–12 tissue regions from four mice. (B) Representative density plots of cytometric analyses from the tissues of WT: LysM-GFP parabionts, gated on Ly6G$^+$ GFP^{HI} neutrophils and showing Annexin V binding in the spleen, bone marrow, liver, and lung. Mean percentages ± SEM of Annexin V$^+$ cells are indicated inside the plots. (C) Experimental design for the transfer of apoptotic thymocytes into wild-type mice, and quantification (bottom) of the percentage of macrophages from various tissues that take up fluorescence. For comparison, the percentages of DsRed$^+$ macrophages found in parabiotic pairs of WT:DsRed-Tg are shown. Bars represent mean ± SEM. *n* = 6 animals per group from two independent experiments.

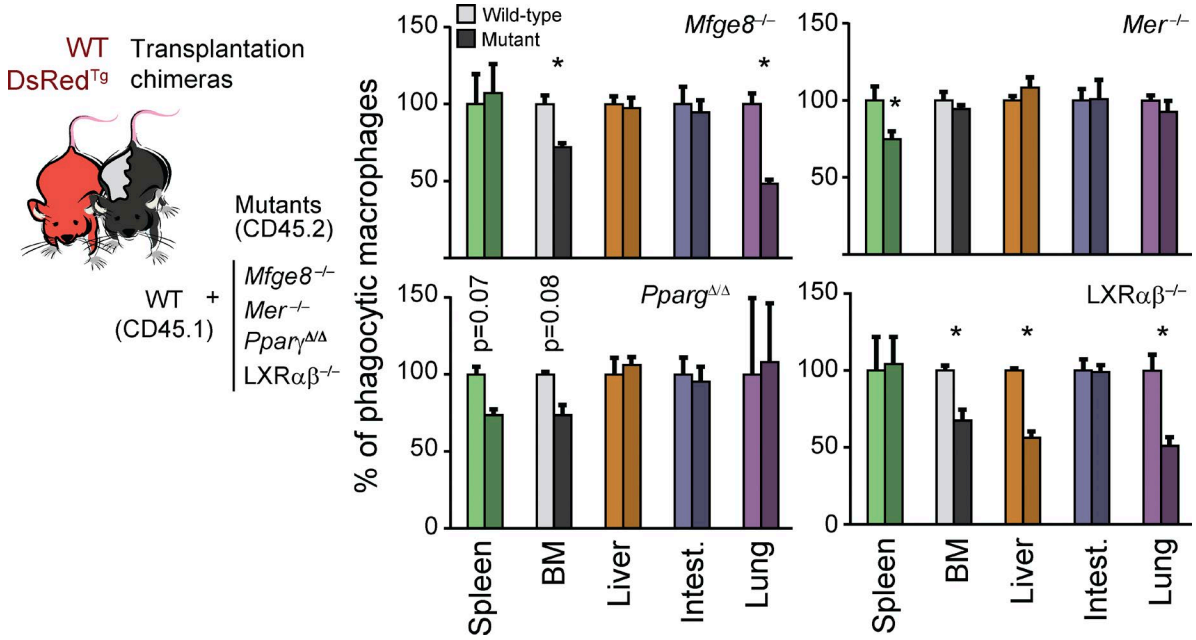

Figure S4. **Phagocytosis by wild-type and mutant macrophages in transplantation chimeras.** Experimental scheme. Mixed chimeras generated by BM transplantation from the indicated mutant (CD45.2) and wild-type (CD45.1) donors were set in parabiosis with DsRed-Tg mice for 4–8 wk. Bar graphs show the relative percentage (normalized to wild-type cells in the same animals) of phagocytic wild-type and mutant macrophages in different tissues. Data are from 3–5 pairs per group from two independent experiments. Bars show mean ± SEM. *, $P < 0.05$, as determined by paired Student's *t* test. Tissues in which there is trend for reduced phagocytosis in mutant mice show the actual P-values.

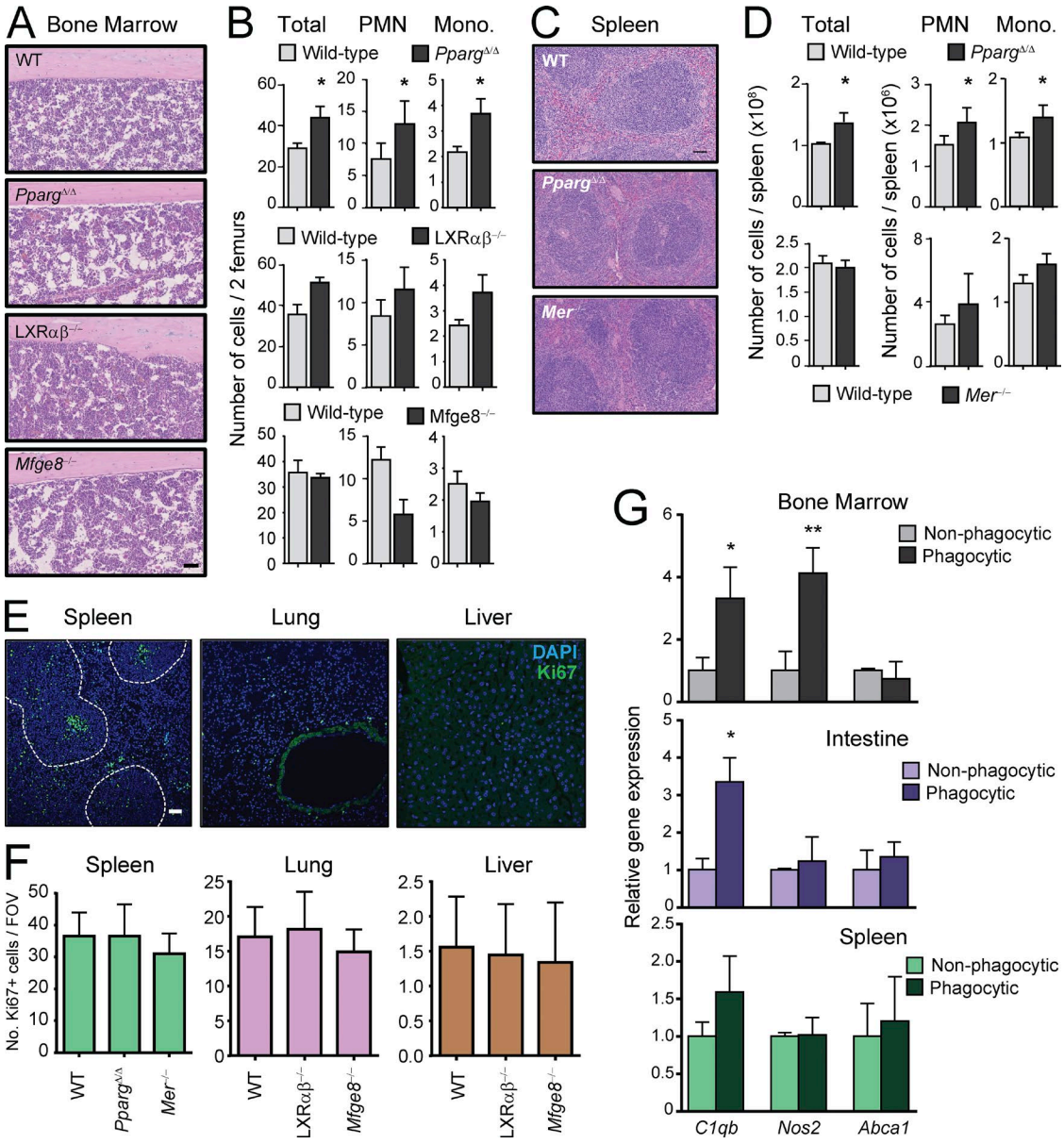

Figure S5. **Tissue-specific mutants show alterations in bone marrow and spleen.** (A) Representative images of hematoxylin/eosin-stained sections of bone marrows from wild-type, *Pparg*$^{\Delta/\Delta}$, LXRαβ$^{-/-}$, and *Mfge8*$^{-/-}$ mice. Bar, 100 µm. (B) Quantification of total bone marrow cellularity, as well as neutrophil and monocytes numbers in the same groups shown in A. *n* = 4–6 mice per group from two independent experiments. (C) Hematoxylin/eosin-stained sections of spleens from *Mer*$^{-/-}$ and *Pparg*$^{\Delta/\Delta}$ mice showing lack of structural alterations in the red pulp compared with wild-type controls. Bar, 100 µm. (D) Total splenocyte, neutrophil, and monocyte counts in the same groups shown in C. *n* = 4–6 mice per group from two independent experiments. Immunofluorescence analysis (E) and quantification (F) of Ki67^{+} cells (green) per field of view in tissue sections from spleen, liver, and lung in the indicated mutants. Bar, 100 µm. Note that many proliferating cells are within white pulps (areas inside dashed lines) but only those in the red pulp were scored for these analyses. No significant differences were found among groups in any tissue. Data are from 10 tissue regions from four mice. (G) Relative expression of genes in phagocytic versus nonphagocytic macrophages isolated from bone marrow, spleen, and intestine of wild-type (CD45.1): DsRed^{Tg} parabionts. *n* = 3–6 mice per group from two independent experiments. Bars show mean ± SEM. *, P < 0.05; **, P < 0.01, as determined by unpaired Student's *t* test analysis.

Table S1. **Diseases and functions predicted for the genes regulated by phagocytosis in bone marrow resident macrophages**

Hematological system development and function, tissue morphology	
Quantity of leukocytes	*ABCA1,AXL,BANK1,BCL2,C1QA,C3AR1,C4A/C4B,CCL5,Ccl9,CCR1,CCR3, CD27,CD38, CD81,CMK LR1,CTSD,CX3CR1,EGR1,GCNT2,GNAS,HEXB,HMOX1,IGF1,IL18BP,IL1B,ITGAD,KITLG,LILRB3,LYN,MERTK,MMP13,NFATC1,PLAC8,RGS1,SER PINB6,SIGLEC1,Srgn,TF,TGFBR2,TIMD4,TIMP2,TLR4, VAV2,VCAM1*
Quantity of blood cells	*ABCA1,AXL,BANK1,BCL2,C1QA,C3AR1,C4A/C4B,CCL5,Ccl9,CCND2,CCR1, CCR3, CD27, CD38, CD81, CMKLR1,CTSD,CX3CR1,EGR1,ENT PD1,GCNT2, GNAS, HEXB, HMOX1, IGF1, IL18BP, IL1B, ITGAD, KITLG, LILRB3, LRP6, LYN, MERTK, MMP13, NFATC1, PLAC8, RGS1, SERPINB6, SIGLEC1, SRGN, TF, TGFBR2, TIMD4, TIMP2, TLR4, VAV2, VCAM1*
Quantity of mononuclear leukocytes	*AXL, BANK1, BCL2, C3AR1, CCL5, CCR1, CCR3, CD27, CD38, CD81, CMKLR1, CTSD, CX3CR1, EGR1, GCNT2, GNAS, HEXB, IGF1, ITGAD, KITLG, LIL RB3, LYN, MERTK, NFATC1, RGS1, SERPINB6, SIGLEC1, TGFBR2, TIMD4, TLR4, VAV2, VCAM1*
Quantity of granulocytes	*C1QA, C3AR1, C4A/C4B, CCR3, CMKLR1, GNAS, IL18BP, IL1B, KITLG, LYN, MMP13, PLAC8, TF, TIMP2, TLR4, VCAM1*
Quantity of myeloid cells	*BCL2, C1QA, C3AR1, C4A/C4B, CCR3, CMKLR1, GNAS, IL18BP, IL1B, KITLG, LYN, MMP13, PLAC8, TF, TIMP2, TLR4, VCAM1*
Quantity of T lymphocytes	*BCL2, CCL5, CCR1, CD27, CMKLR1, CTSD, HEXB, IGF1, ITGAD, KITLG, LYN, MERTK, NFATC1, SERPINB6, SIGLEC1, TGFBR2, TLR4, VAV2, VCAM1*
Hematological system development and function, inflammatory response, tissue morphology	
Quantity of neutrophils	*C1QA, C3AR1, C4A/C4B, CMKLR1, GNAS, IL18BP, IL1B, LYN, MMP13, PLAC8, TF, TIMP2, TLR4, VCAM1*
Quantity of blood platelets	*ABCA1, BCL2, EGR1, ENTPD1, GNAS, IL1B, LYN, TLR4*
Hematological system development and function, immune cell trafficking, inflammatory response, and tissue development	
Accumulation of myeloid cells	*BCL2, CCL5, CCR1, CCR3, CTSC, CX3CR1, EGR1, ENTPD1, GRN, HMOX1, IL1B, ITGAX, TIMP2, TLR4, VCAM1*
Accumulation of leukocytes	*BCL2, C4A/C4B, CCL5, CCR1, CCR3, CD27, CTSC, CX3CR1, EGR1, ENTPD1, GRN, HMOX1, IL1B, ITGAX, TGFBR2, TIMP2, TLR4, VCAM1*
Accumulation of phagocytes	*CCL5, CCR1, CTSC, CX3CR1, EGR1, ENTPD1, GRN, HMOX1, IL1B, ITGAX, TIMP2, TLR4, VCAM1*
Accumulation of macrophages	*CCL5, CCR1, CX3CR1, ENTPD1, GRN, HMOX1, ITGAX, TLR4*
Accumulation of granulocytes	*CCL5, CCR3, CTSC, EGR1, GRN, IL1B, TIMP2, TLR4, VCAM1*
Accumulation of neutrophils	*CTSC, EGR1, GRN, IL1B, TIMP2, TLR4*
Accumulation of mononuclear leukocytes	*BCL2, C4A/C4B, CCL5, CD27, CX3CR1, ENTPD1, TGFBR2, VCAM1*
accumulation of lymphocytes	*BCL2, C4A/C4B, CCL5, CD27, CX3CR1, ENTPD1, VCAM1*

Table S2. **List of primers used for quantitative PCR analyses**

Gene	Forward (5′–3′)	Reverse (3′–5′)
36b4	ACTGGTCTAGGACCCGAGAAG	TCCCACCTTGTCTCCAGTCT
Anxa1	CTTTGCCAAGCCATCCTG	TGGGATGTCTAGTTTCCACCA
C4b	TCTCACAAACCCCTCGACAT	AGCATCCTGGAACACCTGAA
C1qb	CAGGGATAAAGGGGGAGAAA	GGACCCTTAGGGCCAACTT
Ccl2	AGGTGTCCCAAAGAAGCTGTA	ATGTCTGGACCCATTCCTTCT
Ccl9	ACCAGTGGTGGGTGTACCAG	GGTCCGTGGTTGTGAGTTTT
Cd163	TCTCAGTGCCTCTGCTGTCA	CGCCAGTCTCAGTTCCTTCT
Mrc1	CCACAGCATTGAGGAGTTTG	ACAGCTCATCATTTGGCTCA
Cx3cr1	CCATCTGCTCAGGACCTCAC	CAAAATTCTCTAGATCCAGTT CAGG
Ccl19	TGTGGCCTGCCTCAGATTAT	AGTCTTCCGCATCATTAGCAC
Il1b	TGTAATGAAAGACGGCACACC	TCTTCTTTGGGTATTGCTTGG
Nos2	CAGCTGGGCTGTACAAACCTTC	CATTGGAAGTGAAGCGTTTCG
Nr3h1	CAACAGTGTAACAGGCGCT	TGCAATGGGCCAAGGC
Nr3h2	CCCCACAAGTTCTCTGGACACT	TGACGTGGCGGAGGTACTG
Abca1	GGTTTGGAGATGGTTATACAATAG TTGT	CCCGGAAACGCAAGTCC
Mertk	GAGGACTGCTTGGATGAACTGTA	AGGTGGGTCGATCCAAGG
mfge8	GTGCCCTGTGGGCTACTC	GTATTGGGGACGGCTGTG
Pparg	GTGATGGAAGACCACTCGCATT	CCATGAGGGAGTTAGAAGGTTC
Spic	CTGAAAGCCAGCTGGTACAAC	GGTATTCAAACAGCCGAAGC
Tgfb1	CCGAAGCGGACTACTAT	GTAACGCCAGGAATTGT
Vcam1	GACCTGTTCCAGCGAGGGTCTA	CTTCCATCCTCATAGCAATTA AGGTG
Stat4	CGGCATCTGCTAGCTCAGT	TGCCATAGTTTCATTGTTAGA AGC

REFERENCES

Cornelissen, G. 2014. Cosinor-based rhythmometry. *Theor. Biol. Med. Model.* 11:16. http://dx.doi.org/10.1186/1742-4682-11-16

Dzhagalov, I., A. St John, and Y.W. He. 2007. The antiapoptotic protein Mcl-1 is essential for the survival of neutrophils but not macrophages. *Blood.* 109:1620–1626. http://dx.doi.org/10.1182/blood-2006-03-013771

Frenette, P.S., T.N. Mayadas, H. Rayburn, R.O. Hynes, and D.D. Wagner. 1996. Susceptibility to infection and altered hematopoiesis in mice deficient in both P- and E-selectins. *Cell*. 84:563–574. http://dx.doi.org/10.1016/S0092-8674(00)81032-6